

RESEARCH PAPER

Silver-hollow mesoporous silica nanoparticles for clarithromycin delivery in an animal model of *helicobacter pylori*

Sorush Mirfakhraee¹, Reza Mirnejad², Maryam Iman^{3*}

¹Student Research Committee, Baqiyatallah University of Medical Sciences, Tehran, Iran

²Molecular Biology Research Center, Biomedicine Technologies Institute, Baqiyatallah University of Medical Sciences, Tehran, Iran

³Department of Pharmaceutics, Faculty of Pharmacy, Baqiyatallah University of Medical Sciences, Tehran, Iran

ABSTRACT

Background: Nanoparticle-based drug delivery systems offer a promising approach to overcoming antimicrobial resistance and enhancing therapeutic efficacy.

Objective(s): This study aimed to evaluate the efficacy of silver-hollow mesoporous silica nanoparticles (Ag-HMSNs) in the targeted delivery of clarithromycin for eradicating *Helicobacter pylori* (*H. pylori*).

Materials and Methods: A synergistic formulation comprising silver nanoparticles and clarithromycin-loaded hollow mesoporous silica nanoparticles (Ag-HMSNs@CLT) was examined for its antibacterial activity against *H. pylori*. The effectiveness of various anti-*H. pylori* formulations was determined using *in vitro* inhibition assays and *in vivo* bacterial load reduction studies.

Results: The hollow mesoporous silica nanoparticles (HMSNs) demonstrated a high drug-loading capacity, with a clarithromycin content of 27%. The minimum inhibitory concentrations (MIC) for silver nanoparticles (Ag NPs), clarithromycin (CLT), and Ag-HMSNs@CLT were <2 µg/mL, <0.5 µg/mL, and <0.25 µg/mL, respectively. Among the tested formulations, Ag-HMSNs@CLT exhibited the most pronounced reduction in bacterial load during *in vivo* studies and significantly mitigated inflammation, as evidenced by hematoxylin-eosin staining.

Conclusion: The developed nanoparticle-based drug delivery system exhibited excellent drug-loading efficiency and controlled drug release over an extended period. This study highlighted the potential synergistic effects of combining anti-*H. pylori* agents and their efficacy in reducing bacterial growth and alleviating gastrointestinal complications associated with *H. pylori* infection.

Keywords: Drug Release, Drug Delivery Systems, *Helicobacter pylori*, Nanoparticles, Silicon Dioxide

How to cite this article

Mirfakhraee S, Mirnejad R, Iman M. Silver-hollow mesoporous silica nanoparticles for clarithromycin delivery in an animal model of *helicobacter pylori*. *Nanomed J.* 2025; 12(3):433-442. DOI: 10.22038/nmj.2025.81213.2011

INTRODUCTION

Helicobacter pylori (*H. pylori*) is a spiral-shaped bacterium that resides in the stomach lining [1]. This microorganism is recognized as a key factor in the development of various gastrointestinal disorders, including gastritis and peptic ulcers [2]. Its ability to survive in the highly acidic environment of the stomach and evade the host's immune defenses presents significant challenges for effective treatment [3].

Silver nanoparticles (Ag NPs) have emerged as promising agents in combating *H. pylori* infections due to their unique antimicrobial properties [4]. These nanoparticles, typically ranging in size from 1 to 100 nanometers, possess a large surface area and high reactivity [5]. Studies have demonstrated that Ag NPs can disrupt essential microbial processes by binding to bacterial cell walls and compromising membrane integrity [6]. Specifically, Ag NPs have been shown to inhibit the growth and viability of *H. pylori* [7]. Additionally, their ability to induce oxidative stress and cause DNA damage further enhances their antimicrobial efficacy against *H. pylori* [8]. Despite these promising findings, the application of Ag NPs in therapy is

*Corresponding author(s) Email: iman1359@yahoo.com

Note. This manuscript was submitted on July 15, 2024; approved on September 16, 2024

limited by concerns over their toxicity, a challenge similar to that posed by other antibiotics [9–11].

Incorporating Ag NPs into innovative therapeutic strategies holds significant promise for developing effective treatments against *H. pylori* infections and alleviating associated gastrointestinal disorders [12]. Hollow mesoporous silica nanoparticles (HMSNs), known for their non-toxicity, biocompatibility, and high drug-loading capacity, offer particular advantages in this context [13]. The integration of Ag NPs into HMSNs represents a sophisticated and promising avenue in nanomedicine research [14]. HMSNs provide a versatile platform for drug delivery and controlled release due to their high surface area and well-defined pore structure [15]. When combined with Ag nanoparticles, these hybrid nanostructures exhibit enhanced antimicrobial properties, further amplifying their therapeutic potential [16].

Objectives

The mesoporous structure of the silica matrix facilitates the controlled release of antimicrobial drugs, thereby enhancing their efficacy in targeted delivery against microbial infections [17]. This synergistic strategy capitalizes on the advantages of mesoporous silica for drug delivery while simultaneously harnessing the antimicrobial properties of Ag nanoparticles. Such an approach opens new possibilities for innovative applications in combating infections and advancing biomedical treatments [18]. This study was designed to evaluate the response of *H. pylori*-infected rats to clarithromycin loaded into silver-hollow nanoparticles. The findings could contribute to the development of novel therapeutic interventions in gastroenterology.

MATERIALS AND METHODS

Chemicals and reagents

All materials were utilized without further purification and were of analytical grade. Tetraethyl orthosilicate ($\text{Si}(\text{OC}_2\text{H}_5)_4$, TEOS, >99%), bis[3-(triethoxysilyl)propyl]disulfide ($(\text{C}_2\text{H}_5\text{O})_3\text{Si}(\text{CH}_2)_3\text{SS}(\text{CH}_2)_3\text{Si}(\text{OC}_2\text{H}_5)_3$, BTESPD,

>90%), cetyltrimethylammonium chloride ($\text{CH}_3(\text{CH}_2)_{15}\text{N}^+(\text{CH}_3)_3\text{Cl}^-$, CTAC, 50 wt%), triethylamine ($(\text{C}_2\text{H}_5)_3\text{N}$, TEA, >99%), and sodium carbonate (Na_2CO_3) were obtained from Sigma-Aldrich. Clarithromycin (CLT) was generously provided by Tehran Chemie Pharmaceuticals (Tehran, Iran). Silver nanoparticles (99.99% purity) were purchased from Borhan Nano Scale Innovator Company (Mashhad, Iran). Deionized water was used throughout the study.

Synthesis of Hollow Mesoporous Silica Nanoparticles (HMSNs)

The nanoparticles were synthesized following a previously reported method [19]. Briefly, 0.105 mol/L TEOS was added dropwise to a solution containing 46.65 mol/L deionized water, 2.01 mol/L ethanol, and 0.227 mol/L ammonia solution (25%), with stirring for 1 hour. The resulting silica nanoparticles were thoroughly washed with water and ethanol, then centrifuged. These nanoparticles were subsequently added to a mixture of 32.65 mol/L deionized water, 0.326 mol/L CTAC, and 5.7 mmol/L TEA, and the solution was stirred for 24 hours. Following this, 13.8 mmol/L TEOS and 2.87 mmol/L BTESPD were introduced at 80°C, and stirring continued for 1 hour. Selective etching was achieved by adding 0.176 mol/L sodium carbonate at 50°C. Finally, CTAC was removed by repeated dispersion of the nanoparticles in a methanol/NaCl mixture. The HMSNs were freeze-dried for further analysis.

Drug loading of HMSNs

HMSNs (20 mg) were dispersed in a clarithromycin solution in acetone (HMSNs: CLT = 1:2 w/w) and sonicated for 10 minutes. After 72 hours, the mixture was centrifuged, and the supernatant was analyzed using a UV-visible spectrophotometer at 210 nm to quantify the amount of clarithromycin loaded into the HMSNs. The resulting solid was freeze-dried, and the drug loading content and entrapment efficiency were determined using Eqs. (1) and (2), respectively:

$$\text{Loading content (\%)} = \frac{\text{initial amount of clarithromycin (g)} - \text{unloaded clarithromycin (g)}}{\text{weight of clarithromycin loaded nanoparticles (g)}} \times 100 \quad (1)$$

$$\text{Entrapment efficiency (\%)} = \frac{\text{initial amount of clarithromycin} - \text{unloaded clarithromycin}}{\text{initial amount of clarithromycin (g)}} \times 100 \quad (2)$$

Preparation of Ag-HMSNs@CLT

HMSNs@CLT were dispersed in deionized water and sonicated for 10 minutes before being added dropwise to an Ag nanoparticle solution (CLT: Ag =

7.5:2.5 w/w). The mixture was gently stirred for 10 minutes. The resulting silver-decorated HMSNs were then freeze-dried for subsequent testing.

Physicochemical characterization of nanoparticles

The hydrodynamic diameter and zeta potential of the Ag-HMSNs nanoparticles were analyzed using a Malvern Zetasizer Nano ZS via dynamic light scattering (DLS). Absorption spectra were recorded over a 300–700 nm wavelength range using a UV-visible spectrophotometer (UV-1800, Shimadzu). X-ray diffraction (XRD) analysis was performed using an X'Pert Pro diffractometer equipped with a Cu K α radiation source ($\lambda = 1.54 \text{ \AA}$). The morphology of the nanoparticles was examined via transmission electron microscopy (TEM) using a Zeiss EM10 microscope. Prior to imaging, a few drops of the Ag-HMSNs suspension were placed on a carbon-coated copper grid and allowed to dry at room temperature. Scanning electron microscopy (SEM) images were acquired using a VEGA3 microscope at 20 kV after gold coating the samples. The surface area, pore size, and pore volume of the nanoparticles were determined using Brunauer–Emmett–Teller (BET) and Barrett–Joyner–Halenda (BJH) analyses conducted with a BET Mini II instrument.

Drug release test using agar well diffusion method

The in vitro release behavior of clarithromycin was assessed in an acidic medium [5]. The released amount of clarithromycin was measured semi-quantitatively using a microbiological method with *Micrococcus luteus* ATCC 4698 [20]. A precise amount of HMSNs@CLT was redispersed in 1000 mL of pH 1.2 NaCl solution and gently stirred at 37°C in a water bath. Samples of 1 mL were withdrawn and replaced with 1 mL of fresh medium at intervals of 1, 4, and 24 hours. The aliquots were centrifuged, and the supernatants were collected for further analysis. Mueller Hinton agar plates were prepared and inoculated with a 1×10^5 CFU/mL bacterial suspension. Four 6 mm diameter wells were punched into each plate using micropipette tips, and each well was filled with 100 μ L of different test solutions, which were then compared to the control. The plates were incubated at 37°C for 24 hours, after which the average diameter (in millimeters) of the inhibition zones for both the control and the samples was measured. Data were collected in triplicate for each sample.

Minimum Inhibitory Concentration (MIC)

The MICs of HMSNs, CLT, Ag NPs, Ag NPs + CLT, and Ag-HMSNs@CLT against the isolated *H. pylori* strain were determined using the micro broth dilution method in 96-well plates. *H. pylori* was

suspended in Brucella broth supplemented with 5% sheep blood. Ten microliters of broth containing 10^8 CFU/mL of *H. pylori* were added to microplates containing varying concentrations (0.125, 0.250, 0.5, 1, 2, 4, 6, 8, 10, 12, 14, 16, 32, 64 μ g/mL) of each sample. Blank plates without any *H. pylori* culture were used as controls to check for contamination. All plates, including both experimental and control groups, were incubated in a specialized gas incubator at 37°C under a controlled microaerophilic atmosphere (10% CO $_2$, 85% N $_2$, 5% O $_2$) for five days. The OD600 of each well was measured using a microplate reader (Biotek, USA). The lowest concentration that inhibited bacterial growth was recorded as the MIC.

In Vivo H. pylori eradication test

Male Wistar rats (200 g), obtained from the Pasteur Institute of Iran, were used in this study, which was conducted following the protocols approved by the Ethics Committee of Baqiyatullah University of Medical Sciences. *H. pylori* bacteria were cultured on Brucella blood agar (BBA) and harvested by centrifugation at 5,000 rpm for 10 minutes. The bacterial pellet was resuspended in physiological saline to achieve an OD of 1.0 at 590 nm. Each rat was administered 1 mL of this *H. pylori* suspension twice daily via gavage, following overnight fasting and water deprivation, for three consecutive days [21]. After the final administration, the rats were randomly assigned to five groups, with five rats in each group. The first group received normal saline via gavage as a positive control, while the other groups received CLT (7.5 mg/kg), Ag NPs (2.5 mg/kg), CLT + Ag NPs (7.5 mg/kg + 2.5 mg/kg), or Ag-HMSNs@CLT (22.5 mg/kg). One day after treatment, the rats were sacrificed, and their stomachs were immediately removed. Gastric biopsies were washed with saline, fixed in 10% formaldehyde for 24 hours at 4°C, and embedded in paraffin to produce sections. After sample preparation, the BBA medium was incubated at 37°C for 72 hours under microaerobic conditions (10% CO $_2$, 85% N $_2$, 5% O $_2$), followed by colony counting. *H. pylori* colonies were identified by their morphology, Gram-negative staining, and urease test. A gastric tissue section (approximately 5 μ m thick) was stained with hematoxylin-eosin dye to assess tissue inflammation, and all stained sections were examined at 100 \times magnification under a light microscope.

Statistical analysis

The data were analyzed using a one-way ANOVA followed by Tukey's post hoc test in GraphPad Prism 8. A P-value of < 0.05 was considered statistically significant. All experiments were performed in triplicate, and the results are presented as the mean \pm standard deviation (SD).

RESULTS

Preparation and characterization of Ag NPs and HMSNs

The hydrodynamic size of the Ag NPs was determined to be 38 ± 1.15 nm, with a polydispersity index (PDI) of 0.42 ± 0.01 and a zeta potential of -23.2 ± 0.4 mV. Monodispersed hollow mesoporous silica nanoparticles (HMSNs) were prepared via a simple sol-gel method. The HMSNs exhibited a size of 191 ± 10 nm, with a PDI of 0.29 ± 0.03 and a zeta potential of -44 ± 1.5 mV. TEM analysis revealed that HMSNs exhibited a spherical morphology with an average diameter of 150 nm.

Ag NPs, approximately 25 nm in size and cubic, were monodispersely distributed around the HMSNs (Fig. 1A, B). SEM imaging indicated a uniform coating of Ag NPs on spherical HMSNs (Fig. 1C). The BET isotherm exhibited a characteristic type IV adsorption-desorption isotherm, indicative of a mesoporous structure (Fig. 2A). The BET surface area (S_{BET}), pore volume (V_{P}), and BJH pore diameter (V_{BJH}) of the Ag-HMSNs were measured to be $98.19 \text{ m}^2/\text{g}$, $0.49 \text{ cm}^3/\text{g}$, and 3.09 nm, respectively. UV-Vis analysis revealed a broad absorption band centered at approximately 400 nm, corresponding to the presence of Ag NPs (Fig. 2B). The X-ray diffraction (XRD) pattern of the synthesized Ag-HMSNs displayed a broad peak centered around $2\theta = 24^\circ$, indicating the amorphous nature of the HMSNs. In contrast, sharper peaks observed at 38° , 44° , 64° , and 77° were attributed to the crystalline Ag NPs (Fig. 2C).

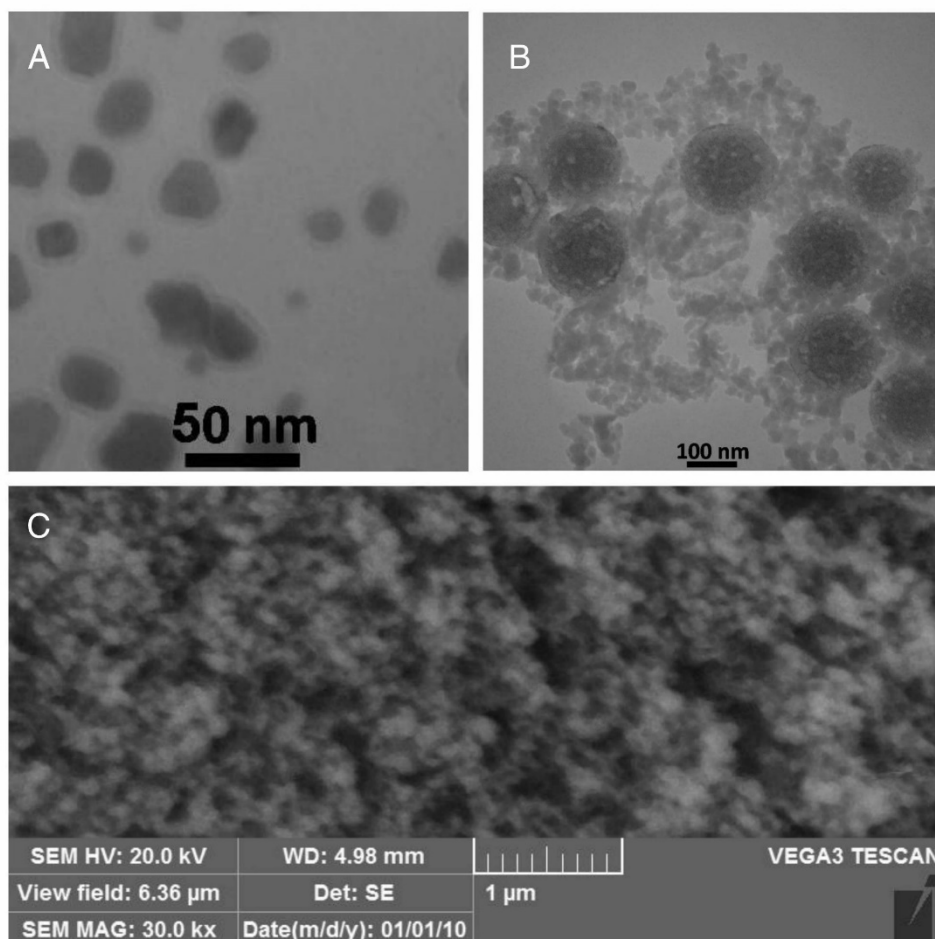


Fig. 1. TEM images of Ag NPs (A), Ag-HMSNs (B), and an SEM image of Ag-HMSNs (C)

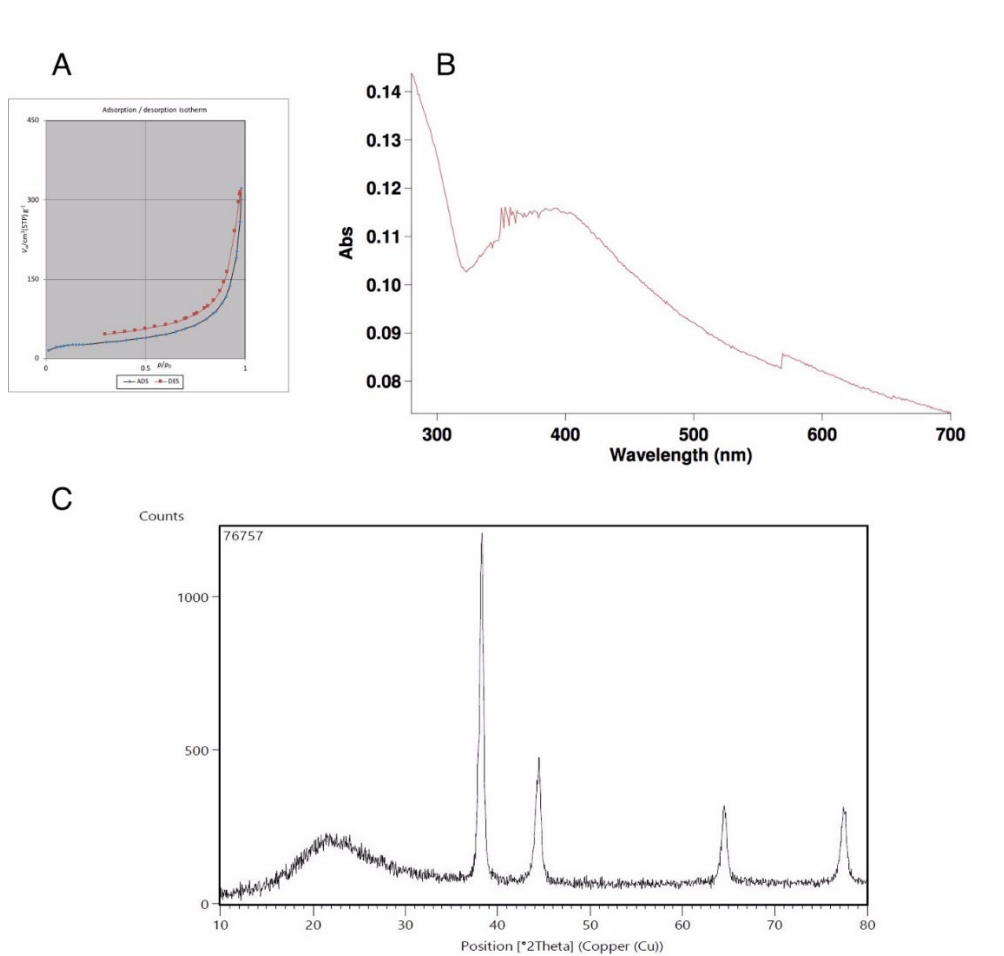


Fig. 2. Nitrogen adsorption-desorption isotherm (A), UV-Vis analysis spectrum (B), and XRD pattern of Ag-HMSNs (C)

Drug loading and release behavior of clarithromycin-loaded HMSNs

The drug loading process was carried out using a straightforward immersion method, with acetone as the solvent, to ensure complete dissolution of clarithromycin. The calculated drug loading content was 27.27%, and the entrapment efficiency was

18.75%. A microbiological assay was employed to evaluate the release of clarithromycin in the medium. No inhibition zones were observed in samples taken at 1 and 4 hours, while distinct zones of inhibition were evident around the wells at 24 hours (Fig. 3).

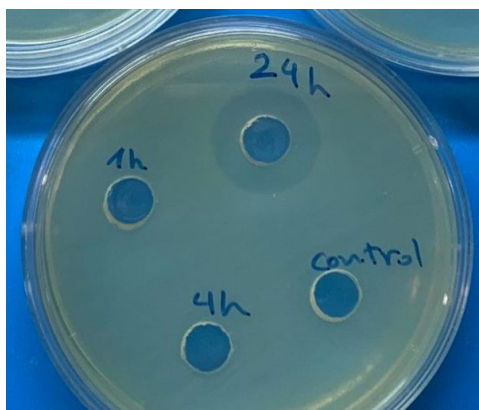


Fig. 3. Disk diffusion assay of clarithromycin release samples against micrococcus luteus.

Anti-*H. pylori* activity of Ag-HMSNs@CLT

A microdilution test was conducted to assess the susceptibility of *H. pylori* to the prepared nanoparticles. The MIC results indicated that *H. pylori* was resistant to HMSNs alone. However, both Ag NPs and CLT exhibited antibacterial activity at concentrations below 2 µg/mL and 0.5 µg/mL, respectively. The combination of Ag NPs + CLT and Ag-HMSNs@CLT was effective at even lower concentrations, specifically 0.25 µg/mL.

In Vivo Anti-*H. Pylori* activity of Ag-HMSNs@CLT

Fig. 4 exhibits the *H. pylori* count following treatment with the control, clarithromycin, AgNPs, Ag + clarithromycin, and Ag-HMSNs@CLT. The average bacterial count for the control group was 17.6×10^5 CFU/stomach. In contrast, the groups treated with CLT, AgNPs, and Ag NPs + CLT exhibited bacterial counts of 8.4×10^5 , 12.4×10^5 , and 9×10^5

CFU/stomach, respectively. The Ag-HMSNs@CLT group demonstrated a significantly lower bacterial count of 2.4×10^5 CFU/stomach.

Hematoxylin-eosin staining was used to detect infiltrated white blood cells in the inflammatory tissue. The staining revealed abundant mononuclear inflammatory cells in the gastric mucosa of the control group, indicative of active gastritis (Fig. 5). A semiquantitative analysis was performed to compare the number of inflammatory cells 24 hours post-treatment. As shown in Figure 6, there was a significant variation in the number of inflammatory cells among the experimental groups. Notably, the Ag-HMSNs@CLT group exhibited the lowest count of inflammatory cells, followed by the CLT, Ag NPs + CLT, and Ag NPs groups. The control group had the highest count of inflammatory cells.

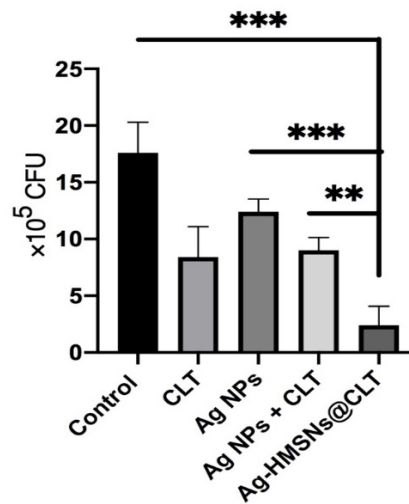


Fig. 4. *H. pylori* bacterial counts measured 24 hours post-treatment. Values are presented as mean ± standard deviation (n = 5). ** and *** indicate a p value < 0.01 and < 0.001, respectively.

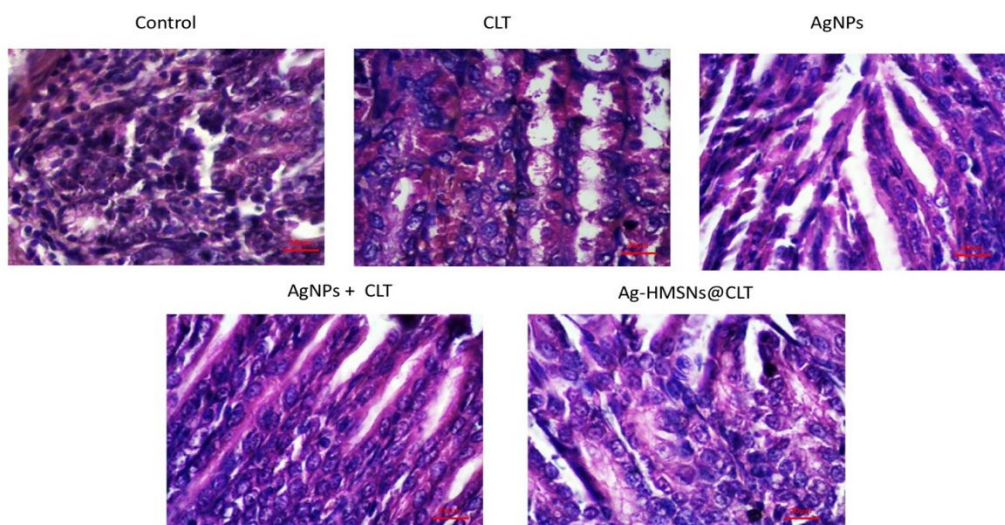


Fig. 5. A comparison of hematoxylin and eosin (H&E) stained gastric tissue among five treatment groups. Scale bar: 20 µm.

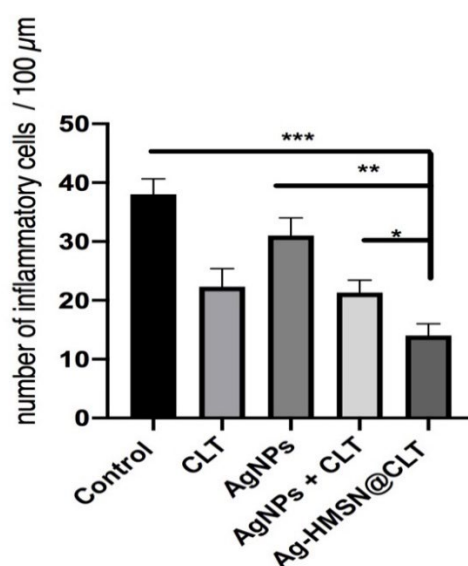


Fig. 6. The number of inflammatory cells in gastric tissues in treatment groups. Values are presented as mean \pm standard deviation (n = 5). * indicates a p value < 0.05.

DISCUSSION

In brief, hollow mesoporous silica nanoparticles were successfully synthesized, loaded with clarithromycin, and decorated with silver nanoparticles. These nanoparticles were selected for their unique properties, including the high loading capacities, stable porous structures of HMSNs, and the robust, broad-spectrum bactericidal properties of Ag NPs [22,23]. The Ag NPs provided an immediate antimicrobial effect, followed by the sustained release of clarithromycin from the HMSNs. TEM images confirmed that the Ag-HMSNs were uniformly dispersed without significant aggregation. Uncoated Ag nanoparticles typically aggregate rapidly in aqueous environments [24]. However, incorporating them into HMSNs has proven to be an effective strategy for preventing aggregation and promoting the controlled release of Ag nanoparticles [25,26]. HMSNs typically exhibit a high surface area, indicative of their mesoporous structure. However, the surface area of Ag-HMSNs was significantly reduced, likely due to the presence of Ag NPs. This reduction in surface area, potentially caused by pore blockage from the Ag nanoparticles, has been observed in previous studies [27,28]. The UV-Vis findings of this study align with those reported by Sampath et al., who synthesized pyrogallol-capped silver nanoparticles exhibiting a surface plasmon resonance (SPR) peak in the 400-500 nm range with a spherical shape and relatively small size [29]. The

XRD results are consistent with previous reports on the XRD patterns of HMSNs and Ag NPs [29,30].

The drug release study indicates that HMSNs can protect clarithromycin from gastric hydrolysis and degradation [31]. Furthermore, HMSNs facilitate the controlled release of encapsulated drugs at the site of infection [32,33]. This controlled release behavior can be attributed to the formation of hydrogen bonds between clarithromycin and the silanol groups within the pores of the silica nanoparticles. For poorly water-soluble drugs, the large surface area and pore volume of HMSNs enable high drug loading and improved dissolution rates [34]. The simple adsorption method used for loading clarithromycin into HMSNs is consistent with previous research on the incorporation of hydrophobic drugs into mesoporous structures [35]. Kabiri et al. studied the loading capacity and release profiles of curcumin as a hydrophobic model drug, reporting a drug loading of 61.57%, with 92.04% of the loaded curcumin released within 6 hours in a simulated plasma model [33].

The MIC results demonstrate that *H. pylori* is resistant to HMSNs alone, primarily serving as a delivery vehicle for clarithromycin. Conversely, Ag NPs alone are effective in eliminating *H. pylori*. In one study, biocompatible silver nanoparticles were synthesized, and the MIC value against *H. pylori* was reported as 18.14 $\mu\text{g}/\text{mL}$, which is higher than the value obtained in our study [36]. This discrepancy may be attributed to differences in the physicochemical properties of the nanoparticles,

such as size, surface charge, morphology, and shape, which influence the interaction between nanoparticles and the bacterial cell wall. Gopinath et al. found that the anti-*H. Pylori* effect of biogenic gold nanoparticles was dependent on both size and bacterial strain, with the bactericidal effect increasing with larger nanoparticle size [37]. Clarithromycin exhibited effectiveness when encapsulated in HMSNs and combined with Ag NPs. Khosravian et al. demonstrated that the antimicrobial activity of clarithromycin-loaded MSNs was superior to that of free clarithromycin against *Staphylococcus aureus* and *Escherichia coli* [13]. The antibacterial properties of nanoparticles are enhanced when combined with antibiotics, and in this study, an additive effect was observed when clarithromycin was combined with Ag nanoparticles. Attia et al. reported that amoxicillin and green-synthesized zinc oxide nanoparticles exhibited synergistic effects when combined in different ratios [38]. Additionally, these findings are supported by the study of Mansouri et al., which showed that Ag NPs reduce the MIC of clarithromycin in both sensitive and resistant strains of *H. pylori* [39].

In vivo, the dosing of clarithromycin was adapted from a standard *H. pylori* treatment regimen and administered based on the weight of the rats [40]. Previous research indicates that Ag NPs' toxicity is dose- and duration-dependent, which led to the administration of a low dose of 2.5 mg/kg [41]. The in vivo results demonstrate that Ag-HMSNs@CLT effectively reduced the bacterial load compared to other treatment groups, highlighting the critical role of the delivery system in eradicating *H. pylori* and emphasizing its importance in achieving therapeutic outcomes. This enhanced effect is likely due to the extended retention of Ag-HMSNs nanoparticles in the stomach, reducing the need for multiple dosing. This finding aligns with the report by Nallasamy et al., which described the preparation of amoxicillin trihydrate and clarithromycin mucoadhesive microspheres. While treatment with free drug solutions achieved a 60% clearance rate of *H. pylori* infection, drug-loaded mucoadhesive microspheres resulted in complete eradication of the infection, likely due to the protective properties of the microspheres and the longer residence time of the loaded drugs [42]. Histopathological analysis indicates that the drug delivery system can modulate inflammatory responses. Ragab and colleagues demonstrated that their combined treatment reduced inflammation and tissue damage caused by *H. pylori* infection in rat stomachs, likely due to a decrease in tumor necrosis factor-alpha (TNF- α)

production, an inflammatory cytokine, in the stomach tissue of infected rats [43]. It is essential to acknowledge the limitations of this study, such as the single-dose administration and the focus on clarithromycin and Ag NPs as treatment options.

CONCLUSION

In summary, the successful fabrication and characterization of clarithromycin-loaded hollow mesoporous-silver nanoparticles demonstrated their potent antibacterial properties against *H. pylori* in both in vitro and in vivo experiments. The study reveals that these nanoparticles exhibit superior efficacy compared to silver nanoparticles, clarithromycin alone, and their simple combination in vivo. These findings highlight the promising potential of our drug delivery system in combating *H. pylori* infections. Future work will explore the antibiofilm activity of Ag-HMSNs@CLT against *H. pylori*.

ACKNOWLEDGMENT

No specific acknowledgments are applicable to this work.

AUTHORS' CONTRIBUTION

S.M. was responsible for data acquisition, data interpretation, and manuscript writing. R.M. and M.I. critically revised the manuscript and supervised the project.

CONFLICT OF INTEREST

The authors declare no conflict of interest.

ETHICAL APPROVAL

The Ethical Committee of Baqiyatallah University of Medical Sciences approved all animal experiments conducted in this study (Ethics Code: IR.BMSU.AEC.1402.033).

FUNDING

The authors confirm that no funding was received for this study.

REFERENCES

- Judaki A, Rahmani A, Feizi J, Asadollahi K, Hafezi Ahmadi MR. Curcumin in combination with triple therapy regimes ameliorates oxidative stress and histopathologic changes in chronic gastritis-associated *Helicobacter pylori* infection. *Arq Gastroenterol.* 2017;54(3):177-182.
- Zhang J, Chen Z, Kong J, Liang Y, Chen K, Chang Y, et al. Fullerene nanoparticles eradicate *Helicobacter pylori*

- via pH-responsive peroxidase activity. *ACS Appl Mater Interfaces*. 2020;12(26).
3. Sutton P, Boag JM. Status of vaccine research and development for *Helicobacter pylori*. *Vaccine*. 2019;37(50):7295-7299.
 4. Al-Bahrani RM, Radif HM, Albaayit SF. Evaluation of potent silver nanoparticles production from *Agaricus bisporus* against *Helicobacter pylori*. *Pak J Agric Sci*. 2020;57:1197-1201.
 5. Almeida Furquim de Camargo B, Soares Silva DE, Noronha da Silva A, Campos DL, Machado Ribeiro TR, Mieli MJ, et al. New silver (I) coordination compound loaded into polymeric nanoparticles as a strategy to improve in vitro anti-*Helicobacter pylori* activity. *Mol Pharm*. 2020;17(7):2287-2298.
 6. Zazo H, Colino CI, Lanao JM. Current applications of nanoparticles in infectious diseases. *J Control Release*. 2016;224:86-102.
 7. Gopalakrishnan V, Masanam E, Ramkumar VS, Baskaraligam V, Selvaraj G. Influence of N-acylhomoserine lactonase silver nanoparticles on the quorum sensing system of *Helicobacter pylori*: A potential strategy to combat biofilm formation. *J Basic Microbiol*. 2020;60(3):207-215.
 8. Pop R, Tăbăran AF, Ungur AP, Negoescu A, Cătoi C. *Helicobacter Pylori*-induced gastric infections: from pathogenesis to novel therapeutic approaches using silver nanoparticles. *Pharmaceutics*. 2022;14(7):1463.
 9. Sampath G, Govarthanan M, Krishnamurthy S, Nagarajan P, Rameshkumar N, Krishnan M, et al. Isolation and identification of metronidazole resistance *Helicobacter pylori* from gastric patients in the southeastern region of India and its advanced antibacterial treatment using biological silver oxide nanoparticles. *Biochem Eng J*. 2022;187:108445.
 10. Amin M, Hameed S, Ali A, Anwar F, Shahid SA, Shakir I, et al. Green synthesis of silver nanoparticles: structural features and in vivo and in vitro therapeutic effects against *Helicobacter pylori* induced gastritis. *Bioinorg Chem Appl*. 2014; (1):135824.
 11. Raza A, Sime FB, Cabot PJ, Maqbool F, Roberts JA, Falconer JR. Solid nanoparticles for oral antimicrobial drug delivery: A review. *Drug Discov Today*. 2019;24(3):858-866.
 12. Lu MM, Ge Y, Qiu J, Shao D, Zhang Y, Bai J, et al. Redox/pH dual-controlled release of chlorhexidine and silver ions from biodegradable mesoporous silica nanoparticles against oral biofilms. *Int J Nanomedicine*. 2018;13:7697-7709.
 13. Khosravian P, Khoobi M, Ardestani MS, Daryasari MP, Hassanzadeh M, Ghasemi-Dehkordi P, et al. Enhancement antimicrobial activity of clarithromycin by amine functionalized mesoporous silica nanoparticles as drug delivery system. *Lett Drug Des Discov*. 2018;15(7):787-795.
 14. Selvarajan V, Obuobi S, Ee PL. Silica nanoparticles—a versatile tool for the treatment of bacterial infections. *Front Chem*. 2020;8:602.
 15. Mirfakhraee S, Bafkary R, Ardakani YH, Dinarvand R. Synthesis of hyaluronic acid-grafted hollow mesoporous silica nanoparticles as nano-carriers for anticancer drug delivery. *J Nanopart Res*. 2022;24(5):100.
 16. Martínez-Carmona M, Gun'ko YK, Vallet-Regí M. Mesoporous silica materials as drug delivery: "The Nightmare" of bacterial infection. *Pharmaceutics*. 2018;10(4):279.
 17. Colilla M, Vallet-Regí M. Targeted stimuli-responsive mesoporous silica nanoparticles for bacterial infection treatment. *Int J Mol Sci*. 2020;21(22):8605.
 18. Gonzalez B, Colilla M, Diez J, Pedraza D, Gueembe M, Izquierdo-Barba I, et al. Mesoporous silica nanoparticles decorated with polycationic dendrimers for infection treatment. *Acta Biomater*. 2018;68:261-271.
 19. Chen F, Hong H, Shi S, Goel S, Valdovinos HF, Hernandez R, et al. Engineering of hollow mesoporous silica nanoparticles for remarkably enhanced tumor active targeting efficacy. *Sci Rep*. 2014;4(1):5080.
 20. Lotfipour F, Valizadeh H, Hallaj-Nezhadi S, Milani M, Zakeri-Milani P. Comparison of microbiological and high-performance liquid chromatographic methods for determination of clarithromycin levels in plasma. *Iran J Pharm Res*. 2010;9(1):27.
 21. Werawatganon D. Simple animal model of *Helicobacter pylori* infection. *World J Gastroenterol*. 2014;20(21):6420.
 22. Frickenstein AN, Hagood JM, Britten CN, Abbott BS, McNally MW, Vopat CA, et al. Mesoporous silica nanoparticles: Properties and strategies for enhancing clinical effect. *Pharmaceutics*. 2021;13(4):570.
 23. Bruna T, Maldonado-Bravo F, Jara P, Caro N. Silver nanoparticles and their antibacterial applications. *Int J Mol Sci*. 2021;22(13):7202.
 24. Li X, Lenhart JJ. Aggregation and dissolution of silver nanoparticles in natural surface water. *Environ Sci Technol*. 2012;46(10):5378-5386.
 25. Tian Y, Qi J, Zhang W, Cai Q, Jiang X. Facile, one-pot synthesis, and antibacterial activity of mesoporous silica nanoparticles decorated with well-dispersed silver nanoparticles. *ACS Appl Mater Interfaces*. 2014;6(15):12038-12045.
 26. He X, Chen F, Chang Z, Waqar K, Hu H, Zheng X, et al. Silver mesoporous silica nanoparticles: fabrication to combination therapies for cancer and infection. *Chem Rec*. 2022;22(4):e202100287.
 27. Montalvo-Quirós S, Gómez-Graña S, Vallet-Regí M, Prados-Rosales RC, González B, Luque-García JL. Mesoporous silica nanoparticles containing silver as novel antimycobacterial agents against *Mycobacterium tuberculosis*. *Colloids Surf B Biointerfaces*. 2021;197:111405.

28. Wang X, Sun W, Yang W, Gao S, Sun C, Li Q. Mesoporous silica-protected silver nanoparticle disinfectant with controlled Ag⁺ ion release, efficient magnetic separation, and effective antibacterial activity. *Nanoscale Adv.* 2019;1(2):840-848.
29. Sampath G, Shyu DJ, Rameshkumar N, Krishnan M, Sivasankar P, Kayalvizhi N. Synthesis and characterization of pyrogallol capped silver nanoparticles and evaluation of their in vitro antibacterial, anti-cancer profile against AGS cells. *J Cluster Sci.* 2021;32:549-557.
30. Purnawira B, Purwaningsih H, Ervianto Y, Pratiwi VM, Susanti D, Rochiem R, et al. Synthesis and characterization of mesoporous silica nanoparticles (MSNp) MCM 41 from natural waste rice husk. *IOP Conf Ser Mater Sci Eng.* 2019;541(1):012018.
31. Li J, Ding Z, Li Y, Miao J, Wang W, Nundlall K, et al. Reactive oxygen species-sensitive thioketal-linked mesoporous silica nanoparticles as drug carrier for effective antibacterial activity. *Mater Des.* 2020;195:109021.
32. Zhang Y, Zhi Z, Jiang T, Zhang J, Wang Z, Wang S. Spherical mesoporous silica nanoparticles for loading and release of the poorly water-soluble drug telmisartan. *J Control Release.* 2010;145(3):257-263.
33. Kabiri F, Mirfakhraee S, Ardakani YH, Dinarvand R. Hollow mesoporous silica nanoparticles for co-delivery of hydrophobic and hydrophilic molecules: mechanism of drug loading and release. *J Nanopart Res.* 2021;23:1-4.
34. Seljak KB, Kocbek P, Gašperlin M. Mesoporous silica nanoparticles as delivery carriers: An overview of drug loading techniques. *J Drug Delivery Sci Technol.* 2020;59:101906.
35. Jafari S, Derakhshankhah H, Alaei L, Fattahi A, Varnamkhasti BS, Saboury AA. Mesoporous silica nanoparticles for therapeutic/diagnostic applications. *Biomed Pharmacother.* 2019;109:1100-1111.
36. Saravanakumar K, Chelliah R, MubarakAli D, Oh DH, Kathiresan K, Wang MH. Unveiling the potentials of biocompatible silver nanoparticles on human lung carcinoma A549 cells and *Helicobacter pylori*. *Sci Rep.* 2019;9(1):5787.
37. Gopinath V, Priyadarshini S, MubarakAli D, Loke MF, Thajuddin N, Alharbi NS, et al. Anti-*Helicobacter pylori*, cytotoxicity and catalytic activity of biosynthesized gold nanoparticles: multifaceted application. *Arab J Chem.* 2019;12(1):33-40.
38. Attia HG, Albarqi HA, Said IG, Alqahtani O, Raey MA. Synergistic effect between amoxicillin and zinc oxide nanoparticles reduced by oak gall extract against *Helicobacter pylori*. *Molecules.* 2022;27(14):4559.
39. Mansouri F, Saffari M, Moniri R, Sedaghat H, Moosavi GA, Molaghanbari M, et al. Investigation of the effect of silver nanoparticles alone and their combination with clarithromycin on *H. pylori* isolates. Available online: <https://assets-eu.researchsquare.com/files/rs-1631922/v1/b64a9332-d940-4409-bb20-8e9716a7ebf8.pdf?c=1660802363> (accessed on 1 September 2024).
40. Villegas I, Rosillo MÁ, Alarcón-de-la-Lastra C, Vázquez-Román V, Llorente M, Sánchez S, et al. Amoxicillin and clarithromycin mucoadhesive delivery system for *helicobacter pylori* infection in a mouse model: Characterization, pharmacokinetics, and efficacy. *Pharmaceutics.* 2021;13(2):153.
41. Hadrup N, Loeschner K, Mortensen A, Sharma AK, Qvortrup K, Larsen EH, et al. The similar neurotoxic effects of nanoparticulate and ionic silver in vivo and in vitro. *Neurotoxicology.* 2012;33(3):416-423.
42. Nallasamy V, Ramanathan S, Perumal P. In vivo evaluation of amoxicillin trihydrate and clarithromycin-loaded mucoadhesive microspheres for *H. pylori* eradication. *Trop J Pharm Res.* 2013;12(2):143-147.
43. Ragab AE, Al-Madboly LA, Al-Ashmawy GM, Saber-Ayad M, Abo-Saif MA. Unravelling the in vitro and in vivo anti-*Helicobacter pylori* effect of delphinidin-3-O-glucoside rich extract from pomegranate exocarp: Enhancing autophagy and downregulating TNF- α and COX2. *Antioxidants.* 2022;11(9):1752.